



Thailand Statistician
January 2026; 24(1): 169-186
<http://statassoc.or.th>
Contributed paper

An ARL Derivation Based on Explicit Formulas to Detect Shifts in the Mean of Seasonal Time-Series Models Running on a CUSUM Control Chart

Wilasinee Peerajit*

Department of Applied Statistics, Faculty of Applied Science, King Mongkut's University of Technology North Bangkok, Bangkok, Thailand.

*Corresponding author; e-mail: wilasinee.p@sci.kmutnb.ac.th

Received: 7 July 2024

Revised: 24 August 2024

Accepted: 27 September 2024

Abstract

Herein, we propose a derivation of the average run length (ARL) to detect shifts in the mean of seasonal time-series models running on a CUSUM control chart based on explicit formulas by solving the Fredholm integral equation of the second kind. The existence and uniqueness of the solution were guaranteed by applying Banach's fixed-point theorem. We applied the explicit formulas for the ARL to detect changes in the mean of a long-memory SARFIMA(p, d, q) \times (P, D, Q) $_s$ process with exponential white noise running on a one-sided CUSUM control chart. When comparing the performance of the proposed method with the ARL obtained via the standard numerical integral equation (NIE) method, the former performed better for small-to-moderate shifts in the process mean under the same conditions and circumstances. Moreover, its percentage accuracy (a benchmark for the ARL) was greater than 95%, thereby indicating excellent agreement between the two methods. In addition, the computer processing time for the proposed method was considerably faster than that required for the NIE method. Hence, this explicit formulas approach provides a novel means of determining the ARL for detecting changes in the mean of a long-memory SARFIMA(p, d, q) \times (P, D, Q) $_s$ process with exponential white noise running on a one-sided CUSUM control chart. Finally, the proposed and NIE methods were applied to applications with real-life data to determine their efficacy.

Keywords: Long-memory SARFIMA process; exponential white noise; numerical integral equation (NIE) method

1. Introduction

In practice, control charts are widely used to monitor changes in a process from an in-control state to an out-of-control state. Since Shewhart (1980) introduced the first control chart, it has become a common practice to utilize them for monitoring assignable cause variations (shifts) in various manufacturing and production processes. The Shewhart control chart is referred to as a memoryless control chart because monitoring using it is not based on previous information. Its main limitation is

that it can only detect large shifts in process parameters. However, memory control charts such as the cumulative sum (CUSUM) control chart (see Page 1954) and exponentially weighted moving average (EWMA) control chart (see Roberts 1959) are incredibly beneficial for detecting small-to-moderate shifts in process parameters.

Montgomery (2004) mentioned that the practical performance of CUSUM and EWMA control charts for detecting continuous changes in a process parameter is quite similar and that neither one has a clear advantage over the other. Hawkins and Wu (2014) conducted a performance comparison of the CUSUM and EWMA control charts. As memory-type charts, both use information from previous observations of the process, and so are sensitive to small shifts in the process parameter (Zwetsloot and Woodall 2017). In the present study, we utilized the CUSUM control chart as it is known for its ability to detect small-to-moderate changes in process parameters. Further information on how to take advantage of the benefits provided by an upper-sided CUSUM control chart can be found in (see Woodall 1984; Brook and Evans 1984; Zacks 1981).

When assessing the performance of control charts, it is usually assumed that observations are independent and identically distributed (i.i.d.) with a normal distribution. However, in practical applications, there are many instances where process data come from non-normal distributions. For example, the data can be autocorrelated, necessitating an appropriate control chart to monitor the process thereon (Vanbrackle and Reynolds 1997; Atienza et al. 2002; Chang and Wu 2011; Sunthornwat et al. 2024).

Autocorrelation involves consecutive data points in a time series that have a propensity to correlate. The goal is to fit the autocorrelated data from the observed process into a time-series model such that observations can be forecasted using the information from the previous observations. The fitted data are then applied to the residuals of the control chart. To monitor autocorrelated processes, the model must offer a framework for designating statistical control. Numerous researchers have thoroughly studied various time-series models, such as autoregressive (AR), moving average (MA), ARMA, AR integrated MA (ARIMA), and AR fractionally integrated MA (ARFIMA). Forecasting models have been used in other disciplines, including economics, finance, meteorology, and astronomy, among others. In the context of time-series analysis, seasonality is a recurring pattern on a monthly, quarterly, or yearly basis.

There has been a growing focus within the field of time-series analysis on models exhibiting long-memory properties. For instance, the properties of the ARFIMA(p, d, q) model when the value of differencing parameter d falls within the range of (0, 0.5) (Granger and Joyeux 1980; Hosking 1981; Hosking 1984). In this context, it affects the hyperbolic decay of the autocorrelation function or the unboundedness of the spectral density function. Conversely, the ARMA model exhibits a decrease in the dependency between observations at a geometric rate. Specifically, we focus on a long-memory process denoted as SARFIMA(p, d, q) \times (P, D, Q) $_s$ with seasonality in the observable data (Porter-Hudak 1990; Ray 1993; Ooms 1995; Montanari et al. 2000) for instance, providing forecasts for IBM product revenues by utilizing a complete SARFIMA(p, d, q) \times (P, D, Q) $_s$ process. Bisognin and Lopes (2009) presented several theoretical properties of SARFIMA(p, d, q) \times (P, D, Q) $_s$ processes, which are time series with periodical long-memory behavior and a finite number of spectral frequencies. Palma (2007) employed the Kalman filter approach to estimate the values of parameters d and D for a SARFIMA(0, $d, 0$) \times (0, $D, 0$) $_s$ process. Since the aforementioned scenario is a common real-world occurrence, we are particularly interested in it within the context of a complete SARFIMA(p, d, q) \times (P, D, Q) $_s$ process while assuming that the white noise follows an exponential

distribution.

One of the most commonly used metrics for control chart performance evaluation is the average run length (ARL), which is the expected number of observations until the first out-of-control signal occurs. It comprises two parts: ARL_0 and ARL_1 . ARL_0 represents the ARL when there is no change in the process parameter (i.e., the in-control process) and should be as large as possible when monitoring the process. In contrast, ARL_1 represents the ARL when there is a change in the process parameter (i.e., the out-of-control process) and should be as small as possible.

There are various methodologies for evaluating the ARL, including Monte Carlo simulation, the Markov chain approach, the numerical integration equation (NIE) method, and the explicit formulas method. For example, Fu and Hu (1999) used Monte Carlo simulation for sensitivity analysis due to its efficiency. Moreover, this method has been studied on charts such as Phantu et al. 2023 and Saengsura et al. 2024. Brook and Evans (1972) proposed the Markov Chain approach to derive the ARL for a process on a CUSUM control chart, as did Lucas and Crosier (1982a) for a two-sided CUSUM control chart. The ARL of a process running on a CUSUM control chart was initially derived using integral equations by Page (1954). Champ and Rigdon (1991) used the Markov Chain approach and the numerical integral equation (NIE) method with the midpoint quadrature rule to approximate the ARL for a process running on CUSUM and EWMA control charts. Sunthornwat (2020) derived explicit formulas for the ARLs of both seasonal and non-seasonal MA processes with exogenous variables running on a CUSUM control chart. Furthermore, the existence and uniqueness of the ARL using explicit formulas can be confirmed by applying Banach's fixed-point theorem (Areepong and Peerajit 2022; Peerajit and Areepong 2023; Peerajit 2023; Sunthornwat and Areepong 2024).

To the best of our knowledge, deriving the ARL for changes in the mean of a $SARFIMA(p, d, q) \times (P, D, Q)_s$ process with exponential white noise running on an upper-sided CUSUM control chart using explicit formulas has not previously been reported. Thus, this became the aim of the present study. After providing the solution for the ARL by solving an integral equation, we carried out a comparison of its efficacy with that using the well-known NIE method. In addition, using the explicit formulas for the ARL to detect a change in the mean of real-life $SARFIMA(p, d, q) \times (P, D, Q)_s$ processes running on an upper-sided CUSUM control chart was also considered.

The remainder of this article is organized as follows. In Section 2, A brief overview of the CUSUM control chart is provided. In Section 3, the $SARFIMA(p, d, q) \times (P, D, Q)_s$ process with exponential white noise is described. In Section 4, an analysis of the solutions for an integral equation using the explicit formulas and NIE methods is provided. In Section 5, the numerical results of a performance comparison of both methods are provided for various scenarios. In Section 6, an example illustrates the use of both methods on real data is given. Finally, conclusions with comments and recommendations for future research are given in Section 7.

2. A Brief Overview of the CUSUM Control Chart for Shifted Process

The one-sided upper CUSUM control chart was considered for this study since an increase in variation is more disadvantageous than a decrease when monitoring a process. Page (1954) suggested the CUSUM control chart for monitoring small-to-moderate shifts in a process parameter. Based on $\{C_t\}$, the plotting statistic for the upper one-sided CUSUM control chart can be defined as follows:

$$C_t = \max \{C_{t-1} + X_t - k, 0\}, \text{ for } t = 1, 2, \dots, \quad (1)$$

where k is the reference parameter of the upper CUSUM control chart and X_t is the sequence of the generalized $SARFIMA(p, d, q) \times (P, D, Q)_s$ process with exponential white noise. Note that $C_0 = \psi$

are the initial values, while the corresponding upper control limit (UCL or h) is constrained by $h \geq \psi$. Moreover, when testing the ARL, the in-control process is usually set as $ARL_0 = 370$. The process is said to be out-of-control when C_t falls outside control limit h ($h \in N$), i.e., $C_t > h$.

According to (1), the corresponding stopping time (τ_h) can be defined as

$$\tau_h = \inf \{t > 0; X_t > h\}, \psi \leq h, \tag{2}$$

where h is the UCL of the upper-sided CUSUM control chart.

3. The SARFIMA Process Running on a CUSUM Control Chart

Here, we investigate the underlying model for the process of interest in this study (SARFIMA(p, d, q) \times (P, D, Q) $_s$ with exponential white noise) running on a CUSUM control chart.

3.1. ARFIMA(p, d, q) model

The ARFIMA model is based on the more familiar Box-Jenkins ARIMA model in which non-integer (fractional) values are allowed for the differencing parameter. Furthermore, it is useful for modeling a time series with an inherent long-memory component (Granger and Joyeux 1980; Hosking 1981; Hosking 1984). In such a series, the rate of decay of the inherent statistical dependence is much slower than the exponential decay typified in a short memory (Box-Jenkins) process. The autocorrelation function of a long-memory process typically decays at a hyperbolic rate (Contreras-Reyes and Palma 2013).

The ARFIMA(p, d, q) process is formulated as:

$$\phi_p(B)(1-B)^d(X_t - \mu) = \theta_q(B)\varepsilon_t, \tag{3}$$

where μ is the mean of the time series, $\phi_p(B)$ and $\theta_q(B)$ are the AR and MA operators with orders p and q , respectively, B refers to the backward operator (i.e., $BX_t = X_{t-1}$), and ε_t is the white noise process. The fractional differencing parameter (d) is stationary and invertible for $d \in (-1, 0.5)$.

3.2. SARFIMA(p, d, q) \times (P, D, Q) $_s$ model

Since our primary interest is long-memory processes with periodicity, we became especially interested in the SARFIMA(p, d, q) \times (P, D, Q) $_s$ model, which is an extension of the ARFIMA(p, d, q) model.

In a particular case of SARFIMA(p, d, q) \times (P, D, Q) $_s$ where $p = q = P = Q = 0$, with fractional values $d, D \in \mathbb{R}^2$, the process can be expressed as follows:

$$(1-B)^d(1-B^S)^D X_t = \varepsilon_t, t \in \mathbb{Z}, \tag{4}$$

where $\varepsilon_t \sim Exp(\lambda)$ of particular interest is the SARFIMA(p, d, q) \times (P, D, Q) $_s$ model of a long-memory process where the non-seasonal and seasonal fractionally differenced parameters d and D , respectively, are between 0 and 0.5.

For all $\partial = (d, D)$, and both non-seasonal and seasonal filters can be computed via the binomial expansion as follows,

$$(1-B^\nu)^\partial := \sum_{\ell=0}^{\infty} \binom{\partial}{\ell} (-1)^\ell (B^\nu)^\ell = 1 - \partial B^\nu - \frac{1}{2!} \partial(\partial-1) B^{2\nu} - \dots, \tag{5}$$

and

$$v = \begin{cases} 1 & ; \text{for operator } d \\ S \in \mathbb{N} \setminus \{0, 1\} & ; \text{for operator } D, \end{cases}$$

where $\binom{\partial}{\ell} = \frac{\Gamma(1+\partial)}{\Gamma(1+\ell)\Gamma(1+\partial-\ell)}$, and $\Gamma(\cdot)$ is the gamma function.

The SARFIMA(p, d, q) \times (P, D, Q) $_S$ for X_t can be expressed in following form:

$$\phi_p(B)\Phi_p(B^S)(1-B)^d(1-B^S)^D X_t = \theta_q(B)\Theta_Q(B^S)\varepsilon_t, \tag{6}$$

where $\phi_p(B)$, and $\theta_q(B)$ are non-seasonal AR and MA polynomials in B of order p and q respectively, $\Phi_p(B^S)$ and $\Theta_Q(B^S)$ are seasonal AR and MA polynomials in B of order P and Q , respectively. It can be respectively expressed as follows:

$$\phi_p(B) = (1 - \phi_1 B - \phi_2 B^2 - \dots - \phi_p B^p), \theta_q(B) = (1 - \theta_1 B - \theta_2 B^2 - \dots - \theta_q B^q),$$

$$\Phi_p(B^S) = (1 - \Phi_1 B^S - \Phi_2 B^{2S} - \dots - \Phi_p B^{pS}), \text{ and } \Theta_Q(B^S) = (1 - \Theta_1 B^S - \Theta_2 B^{2S} - \dots - \Theta_Q B^{QS}).$$

Interestingly, ε_t represents white noise with exponential distribution; $\varepsilon_t \sim \text{Exp}(\lambda)$ (Suparman 2018, Peerajit 2022). Meanwhile, S is the number of time periods in a year; e.g., $S = 12$ for a monthly series. Restricting SARFIMA(p, d, q) \times (P, D, Q) $_S$ to take only non-integer values would simplify it to an ARFIMA model.

Finally, (5) and (6) can be rearranged to emphasize the case $p = q = P = Q = 1, S = 12$ for fractional values of parameters $d, D \in (0, 0.5)$. In this case, the process can be expressed as

$$X_t = \varepsilon_t - \theta_1 \varepsilon_{t-1} - \Theta_1 \varepsilon_{t-12} + \theta_1 \Theta_1 \varepsilon_{t-13} + \phi_1 X_{t-1} M + \Phi_1 X_{t-12} M - \phi_1 \Phi_1 X_{t-13} M, \tag{7}$$

where $M = (1 - dB - \frac{d(1-d)B^2}{2} - \dots)(1 - DB^{12} - \frac{D(1-D)B^{12}}{2} - \dots)$, and X_t denoted as generalized SARFIMA($1, d, 1$) \times ($1, D, 1$) $_{12}$ process with exponential white noise applied to run on a CUSUM control chart. For all initial values for the SARFIMA($1, d, 1$) \times ($1, D, 1$) $_{12}$ process is are equal to 1. where $-1 \leq \phi_1, \theta_1 \leq 1$ are non-seasonal AR and MA coefficients and $-1 \leq \Phi_1, \Theta_1 \leq 1$ are seasonal AR and MA coefficients.

4. Methods to Derive the ARL for Shifts in the Mean of a SARFIMA Process Running on a CUSUM Control Chart

Here, we show derivations of ARL using explicit formulas (i.e., the proposed method) and the NIE method.

4.1. Derivation of the ARL Using Explicit Formulas

To begin with, (1) and (7) can be rearranged to provide recursion of the CUSUM statistic for a long-memory SARFIMA(p, d, q) \times (P, D, Q) $_{12}$ process to provide

$$C_t = C_{t-1} + \varepsilon_t - \theta_1 \varepsilon_{t-1} - \Theta_1 \varepsilon_{t-12} + \theta_1 \Theta_1 \varepsilon_{t-13} + \phi_1 X_{t-1} M + \Phi_1 X_{t-12} M - \phi_1 \Phi_1 X_{t-13} M - k, \tag{8}$$

where $\varepsilon_t \sim \text{Exp}(\lambda)$.

The control limits in this instance are LCL = 0, CL = λ , and UCL = h . For $0 < C_t < h$, we obtain

$$\begin{bmatrix} \theta_1 \varepsilon_{t-1} + \Theta_1 \varepsilon_{t-2} - \theta_1 \Theta_1 \varepsilon_{t-3} - \phi_1 X_{t-1} M \\ -\Phi_1 X_{t-2} M + \phi_1 \Phi_1 X_{t-3} M + k - C_{t-1} \end{bmatrix} < \varepsilon_t < \begin{bmatrix} h + \theta_1 \varepsilon_{t-1} + \Theta_1 \varepsilon_{t-2} - \theta_1 \Theta_1 \varepsilon_{t-3} - \phi_1 X_{t-1} M \\ -\Phi_1 X_{t-2} M + \phi_1 \Phi_1 X_{t-3} M + k - C_{t-1} \end{bmatrix},$$

where $C_0 = \psi$; $\psi \in (0, h]$. According to the stopping time (τ_h) in (2), the ARL can be defined as

$$ARL = L(\psi) = E_m(\tau_h).$$

Let $\varepsilon_t, t = 1, 2, \dots$, be a sequence of continuous i.i.d. random variables with an exponential distribution. Therefore, $L(\psi)$ can be used to solve the integral equation using the Fredholm integral equation of the second kind as follows:

$$L(\psi) = 1 + L(0)F(k - \psi - X_t) + \int_0^h L(y)f(y + k - \psi - X_t)dy, \tag{9}$$

where $F(\cdot)$ and $f(\cdot)$ are the cumulative distribution function (cdf) and probability density function (pdf) of an exponential distribution, respectively. Hence, (9) can be rewritten as

$$\begin{aligned} L(\psi) = & 1 + L(0) \left(1 - \exp \left\{ \begin{matrix} -\lambda(k - \psi + \theta_1 \varepsilon_{t-1} + \Theta_1 \varepsilon_{t-2} - \theta_1 \Theta_1 \varepsilon_{t-3}) \\ -\phi_1 X_{t-1} M + \Phi_1 X_{t-2} M + \phi_1 \Phi_1 X_{t-3} M \end{matrix} \right\} \right) \\ & + \lambda \left(\exp \left\{ \begin{matrix} \lambda(\psi - k - \theta_1 \varepsilon_{t-1} - \Theta_1 \varepsilon_{t-2} + \theta_1 \Theta_1 \varepsilon_{t-3}) \\ +\phi_1 X_{t-1} M + \Phi_1 X_{t-2} M - \phi_1 \Phi_1 X_{t-3} M \end{matrix} \right\} \right) \int_0^h L(y) \exp\{-\lambda y\} dy. \end{aligned} \tag{10}$$

To simplify the formulation, we define $g = \int_0^h L(y) \exp\{-\lambda y\} dy$, according to (10) as follows:

$$L(\psi) = 1 + L(0) \left(1 - \exp \left\{ \begin{matrix} -\lambda(k - \psi + \theta_1 \varepsilon_{t-1} + \Theta_1 \varepsilon_{t-2}) \\ -\theta_1 \Theta_1 \varepsilon_{t-3} - \phi_1 X_{t-1} M \\ +\Phi_1 X_{t-2} M + \phi_1 \Phi_1 X_{t-3} M \end{matrix} \right\} \right) + \lambda \left(\exp \left\{ \begin{matrix} \lambda(\psi - k - \theta_1 \varepsilon_{t-1} - \Theta_1 \varepsilon_{t-2}) \\ +\theta_1 \Theta_1 \varepsilon_{t-3} + \phi_1 X_{t-1} M \\ +\Phi_1 X_{t-2} M - \phi_1 \Phi_1 X_{t-3} M \end{matrix} \right\} \right) g. \tag{11}$$

By replacing $\psi = 0$ in (11), we obtain

$$\begin{aligned} L(0) = & 1 + L(0) \left(1 - \exp \left\{ \begin{matrix} -\lambda(k - \psi + \theta_1 \varepsilon_{t-1} + \Theta_1 \varepsilon_{t-2}) \\ -\theta_1 \Theta_1 \varepsilon_{t-3} - \phi_1 X_{t-1} M \\ +\Phi_1 X_{t-2} M + \phi_1 \Phi_1 X_{t-3} M \end{matrix} \right\} \right) + \lambda g \left(\exp \left\{ \begin{matrix} \lambda(\psi - k - \theta_1 \varepsilon_{t-1} - \Theta_1 \varepsilon_{t-2}) \\ +\theta_1 \Theta_1 \varepsilon_{t-3} + \phi_1 X_{t-1} M \\ +\Phi_1 X_{t-2} M - \phi_1 \Phi_1 X_{t-3} M \end{matrix} \right\} \right) \\ L(0) = & \exp \left\{ \begin{matrix} \lambda(\psi - k - \theta_1 \varepsilon_{t-1} - \Theta_1 \varepsilon_{t-2} + \theta_1 \Theta_1 \varepsilon_{t-3}) \\ +\phi_1 X_{t-1} M + \Phi_1 X_{t-2} M - \phi_1 \Phi_1 X_{t-3} M \end{matrix} \right\} + \lambda g. \end{aligned} \tag{12}$$

After substituting $L(0)$ from (12) into (11), it follows that

$$L(\psi) = 1 + \lambda g + \exp \left\{ \begin{matrix} \lambda(k + \theta_1 \varepsilon_{t-1} + \Theta_1 \varepsilon_{t-2} - \theta_1 \Theta_1 \varepsilon_{t-3}) \\ -\phi_1 X_{t-1} M + \Phi_1 X_{t-2} M + \phi_1 \Phi_1 X_{t-3} M \end{matrix} \right\} - \exp\{\lambda \psi\}. \tag{13}$$

Subsequently, constant g can be defined as

$$\begin{aligned} g = & \int_0^h L(y) \exp\{-\lambda y\} dy = \int_0^h (1 + \lambda g + \exp \left\{ \begin{matrix} \lambda(k + \theta_1 \varepsilon_{t-1} + \Theta_1 \varepsilon_{t-2} - \theta_1 \Theta_1 \varepsilon_{t-3}) \\ -\phi_1 X_{t-1} M + \Phi_1 X_{t-2} M + \phi_1 \Phi_1 X_{t-3} M \end{matrix} \right\} - \exp\{\lambda y\}) \exp\{-\lambda y\} dy \\ g = & \frac{\exp\{\lambda h\}}{\lambda} (1 + \exp \left\{ \begin{matrix} \lambda(k + \theta_1 \varepsilon_{t-1} + \Theta_1 \varepsilon_{t-2} - \theta_1 \Theta_1 \varepsilon_{t-3}) \\ -\phi_1 X_{t-1} M + \Phi_1 X_{t-2} M + \phi_1 \Phi_1 X_{t-3} M \end{matrix} \right\}) \cdot (1 - \exp\{-\lambda h\}) - h \exp\{\lambda h\}. \end{aligned} \tag{14}$$

Finally, substituting constant g from Equation (14) into Equation (13) results in

$$L(\psi) = \exp\{\lambda h\} \left(1 + \exp \left\{ \begin{matrix} \lambda(k + \theta_1 \varepsilon_{t-1} + \Theta_1 \varepsilon_{t-2} - \theta_1 \Theta_1 \varepsilon_{t-3}) \\ -\phi_1 X_{t-1} M + \Phi_1 X_{t-2} M + \phi_1 \Phi_1 X_{t-3} M \end{matrix} \right\} - \lambda h \right) - \exp\{\lambda \psi\}; \quad \psi \geq 0. \quad (15)$$

This is the ARL derived using the explicit formulas. Next, we prove its existence and uniqueness by applying Banach’s fixed-point theorem.

Theorem 1. Banach’s fixed-point theorem

Let (M, d) be a complete metric space and $T : M \rightarrow M$ be the contraction mapping on M , then $\omega \in [0, 1)$ exists when

$$d(T(L_1), T(L_0)) \leq \omega d(L_1, L_0) \text{ for all } L_1, L_0 \in M.$$

where T has a precisely unique fixed point $L(\cdot) \in M$ such that $T(L) = L$.

Proof: (Existence).

Let T be a contraction in complete metric space (M, d) and $C([0, h])$ be a set of continuous functions of $L(\psi)$ on interval $([0, h])$, then L can be obtained by starting with arbitrary element $L_0 \in C([0, h])$ and then defining sequence $\{L_n\}_{n \geq 0}$ and sequence $L_n = T(L_{n-1})$ for $n \geq 0$. Hence, we obtain inequality

$$d(L_{n+1}, L_n) \leq \omega^n d(L_1, L_0).$$

Now, we show that $\{L_n\}_{n \in \mathbf{N}}$ is a Cauchy sequence. Let $m, n \in \mathbf{N}$ such that $m > n$:

$$\begin{aligned} d(L_m, L_n) &\leq d(L_m, L_{m-1}) + d(L_{m-1}, L_{m-2}) + \dots + d(L_{n+1}, L_n) \\ &\leq \omega^{m-1} d(L_1, L_0) + \omega^{m-2} d(L_1, L_0) + \dots + \omega^n d(L_1, L_0) \\ &= \frac{\omega^n}{1 - \omega} d(L_1, L_0). \end{aligned}$$

Thus, since $\{L_n\}_{n \geq 0}$ is a Cauchy sequence and $\lim_{n \rightarrow \infty} T^n(L_n) \rightarrow L$, we can conclude that $T(L) = L$.

Proof: (Uniqueness).

Let L_1 and L_2 be two arbitrary functions in $C([0, h])$, and $k(\psi, y)$ is a kernel function of $(L(\psi))$, where

$$k(\psi, y) = \exp \left\{ \begin{matrix} \lambda(\psi - k - \theta_1 \varepsilon_{t-1} - \Theta_1 \varepsilon_{t-s} + \theta_1 \Theta_1 \varepsilon_{t-(s+1)}) \\ +\phi_1 X_{t-1} M + \Phi_1 X_{t-s} M - \phi_1 \Phi_1 X_{t-(s+1)} M \end{matrix} \right\} \lambda \exp\{-\lambda y\} \text{ and } k : [0, h] \times [0, h] \rightarrow \mathbf{R}.$$

Inequality $\sup_{\psi \in [0, h]} \int_0^h |k(\psi, y)| dy < 1$ can be used to prove that T is a contraction mapping on complete metric space $(C([0, h]), \|\cdot\|_\infty)$.

$$\begin{aligned} \|T(L_1) - T(L_2)\|_\infty &= \sup_{\psi \in [0, h]} \int_0^h \exp \left\{ \frac{\lambda(\psi - k - \theta_1 \varepsilon_{t-1} - \Theta_1 \varepsilon_{t-S} + \theta_1 \Theta_1 \varepsilon_{t-(S+1)})}{+\phi_1 X_{t-1} M + \Phi_1 X_{t-S} M - \phi_1 \Phi_1 X_{t-(S+1)} M} \right\} \lambda \exp \{-\lambda y\} \cdot |L_1(y) - L_2(y)| dy \\ &\leq \sup_{\psi \in [0, h]} \int_0^h \exp \left\{ \frac{\lambda(\psi - k - \theta_1 \varepsilon_{t-1} - \Theta_1 \varepsilon_{t-S} + \theta_1 \Theta_1 \varepsilon_{t-(S+1)})}{+\phi_1 X_{t-1} M + \Phi_1 X_{t-S} M - \phi_1 \Phi_1 X_{t-(S+1)} M} \right\} \lambda \exp \{-\lambda y\} dy \cdot \|L_1(y) - L_2(y)\|_\infty \\ &\leq \omega \|L_1(y) - L_2(y)\|_\infty \end{aligned}$$

where $\omega = \sup_{\psi \in [0, h]} \int_0^h \exp \left\{ \frac{\lambda(\psi - k - \theta_1 \varepsilon_{t-1} - \Theta_1 \varepsilon_{t-S} + \theta_1 \Theta_1 \varepsilon_{t-(S+1)})}{+\phi_1 X_{t-1} M + \Phi_1 X_{t-S} M - \phi_1 \Phi_1 X_{t-(S+1)} M} \right\} \lambda \exp \{-\lambda y\} dy < 1$ Thus, $L(\psi)$ exists

and is unique.

The ARL of the in-control process (ARL₀) with exponential parameter $\lambda = \lambda_0$ can be obtained by

$$ARL_0 = \exp \{ \lambda_0 h \} \left(1 + \exp \left\{ \frac{\lambda_0 (k + \theta_1 \varepsilon_{t-1} + \Theta_1 \varepsilon_{t-12} - \theta_1 \Theta_1 \varepsilon_{t-13})}{-\phi_1 X_{t-1} M + \Phi_1 X_{t-12} M + \phi_1 \Phi_1 X_{t-13} M} \right\} - \lambda_0 h \right) - \exp \{ \lambda_0 \psi \}. \tag{16}$$

The explicit formulas for the out-of-control ARL (ARL₁) can be evaluated similarly. Here, we assume that a shift in the process mean can be defined as

$$\lambda_1 = \lambda_0 (1 + \delta),$$

where δ is a specified constant. Hence, the out-of-control ARL after a shift in the process mean is given by

$$ARL_1 = \exp \{ \lambda_1 h \} \left(1 + \exp \left\{ \frac{\lambda_1 (k + \theta_1 \varepsilon_{t-1} + \Theta_1 \varepsilon_{t-12} - \theta_1 \Theta_1 \varepsilon_{t-13})}{-\phi_1 X_{t-1} M + \Phi_1 X_{t-12} M + \phi_1 \Phi_1 X_{t-13} M} \right\} - \lambda_1 h \right) - \exp \{ \lambda_1 \psi \}. \tag{17}$$

The preceding equation reveals a computationally easy formula that uses ARL₁ based on explicit formulas to detect a shift in the process mean of a long-memory SARFIMA(p, d, q) × (P, D, Q)_s with exponential white noise running on a CUSUM control chart.

4.2. Approximation of the ARL using the NIE method

This can be achieved by applying a quadrature rule (Atkinson and Han 2001; Sukparungsee and Areepong 2017) as follows:

$$\int_0^h W(y)F(y) dy \approx \sum_{j=1}^m w_j F(u_j),$$

where $W(y)$ and $F(y)$ are given functions, u_j is a set of points, and w_j is a weight depending on the quadrature rule applied. Let $\hat{L}(\psi)$ denotes the approximation $L(\psi)$ on interval $[0, h]$ by substituting ψ with u_i ; $i = 1, 2, \dots, m$ in (10) using the quadrature rule to give

$$\hat{L}(u_i) = 1 + \hat{L}(u_i) F \left\{ \frac{k - u_i + \theta_1 \varepsilon_{t-1} + \Theta_1 \varepsilon_{t-12}}{-\theta_1 \Theta_1 \varepsilon_{t-13} - \phi_1 X_{t-1} M} \right. \left. + \sum_{j=1}^m w_j \hat{L}(u_j) f \left\{ \frac{k + u_j - u_i + \theta_1 \varepsilon_{t-1} + \Theta_1 \varepsilon_{t-12}}{+\Phi_1 X_{t-12} M + \phi_1 \Phi_1 X_{t-13} M} \right\} \right\}.$$

See details of the proof in Bualuang and Peerajit (2022). Therefore, the NIE method for the ARL to detect changes in the mean of a SARFIMA(1, $d, 1$) × (1, $D, 1$)_s process running on a CUSUM control chart can be defined as

$$\hat{L}(\psi) = 1 + \hat{L}(u_1)F \left\{ \begin{matrix} k - \psi + \theta_1 \varepsilon_{t-1} + \Theta_1 \varepsilon_{t-12} \\ -\theta_1 \Theta_1 \varepsilon_{t-13} - \phi_1 X_{t-1} M \\ + \Phi_1 X_{t-12} M + \phi_1 \Phi_1 X_{t-13} M \end{matrix} \right\} + \sum_{j=1}^m w_j \hat{L}(u_j) f \left(\begin{matrix} k + u_j - \psi + \theta_1 \varepsilon_{t-1} + \Theta_1 \varepsilon_{t-12} \\ -\theta_1 \Theta_1 \varepsilon_{t-13} - \phi_1 X_{t-1} M \\ + \Phi_1 X_{t-12} M + \phi_1 \Phi_1 X_{t-13} M \end{matrix} \right), \quad (18)$$

with $w_j = \frac{h}{m}$, and $u_j = \frac{h}{m} \left(j - \frac{1}{2} \right); j = 1, 2, \dots, m$. This method was used to verify the accuracy of ARL derived using explicit formulas in the numerical study.

5. Performance Evaluation and Comparison

We computed the ARL using (16)-(18) via the Mathematica software based on the Wolfram functional programming language. For the ARL derived using the NIE method, we set the number of division points $m = 800$. The reference parameter (k) was set as 2.5, 3.5, or 4.5. We computed the UCL (h) in conjunction with k by utilizing (16) so that $ARL_0 \approx 370$. Three SARFIMA(p, d, q) $\times (P, D, Q)_s$ models were considered: SARFIMA(1, $d=0.25, 1$) $\times (1, 0.1, 1)_{12}$, SARFIMA(1, $d = 0.35, 1$) $\times (1, 0.1, 1)_{12}$ and SARFIMA(1, $d=0.45, 1$) $\times (1, 0.1, 1)_{12}$, with coefficient parameters $\phi_1 = 0.1$, $\theta_1 = 0.1$, $\Phi_1 = 0.1$, and $\Theta_1 = 0.1$. For the exponential white noise ($\varepsilon_t \sim Exp(\lambda)$), several scenarios of the exponential parameters were considered: ($\lambda = \lambda_0$), $\lambda_0 = 1$, and for the out-of-control process, ($\lambda = \lambda_1$) equals $\lambda_1 = \lambda_0(1 + \delta)$ for shift sizes ($\delta > 0$) of 0.025, 0.05, 0.10, 0.25, 0.50, 0.75, 1, 2, 3, 4, or 5. The shift sizes were categorized as small-to-moderate ($0 < \delta \leq 0.5$) or large ($0.5 < \delta \leq 5$). More details are provided in the following subsections.

5.1. The in-control process

The ideal in-control process comprises $ARL_0 = 370$ and a shift size of 0. For the three models mentioned in the previous section and using $k = 2.5, 3.5, 4.5$ and $UCL(h) = 4.14452, 2.793457, 1.728737$, $ARL_0 = 370$ can be assigned to the CUSUM control chart running a SARFIMA(1, $d = 0.25, 1$) $\times (1, D = 0.1, 1)_{12}$ process. The bar charts in Figure 1 show that as k was increased, the UCL decreased.

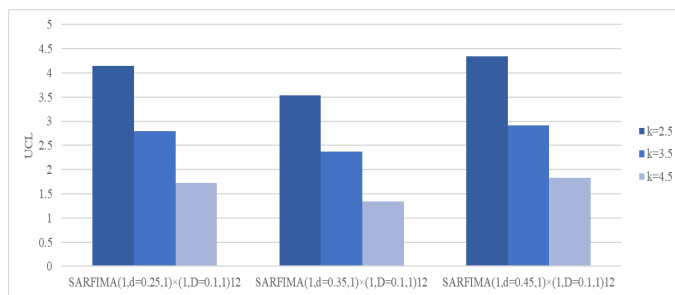


Figure 1 The UCLs for the three models running on a CUSUM control chart after assigning various values of (k) and $ARL_0 = 370$

5.2 The out-of-control process

We examined the performances of the ARL derivations using the proposed and NIE methods to detect changes in the means of the SARFIMA(p, d, q) $\times (P, D, Q)_s$ processes with exponential white

noise mentioned earlier running on a CUSUM control chart. The results in Tables 1–3 report their out-of-control performances. Furthermore, the results using both methods are compared using the following metric:

$$\% \text{ Accuracy} = 100 - \left| \frac{\mathcal{L}(\psi) - \hat{\mathcal{L}}(\psi)}{\mathcal{L}(\psi)} \right| \times 100\%, \tag{19}$$

where $\mathcal{L}(\psi)$ and $\hat{\mathcal{L}}(\psi)$ are the ARL values obtained from the explicit formulas and NIE methods, respectively. A percentage accuracy of greater than 95% indicates excellent agreement between the two methods.

It can be seen that the out-of-control ARL results calculated using the explicit formulas are close to those using the NIE method in all cases considered. Moreover, the percentage accuracy results were 99% or thereabouts in all cases, thereby inferring that the results are in excellent agreement and the proposed method is very accurate. The ARL_1 results calculated using both methods decreased rapidly with increasing shift size, thereby indicating that they are more effective at detecting small-to-moderate shifts than large ones. As can be seen in Figure 2, $k=2.5$ yielded the lowest ARL_1 values for all three models. Finally, the computation time required for the explicit formulas to carry out the calculation was only a fraction of a second while that of the NIE method was 1,800-1,900 seconds.

Overall, the results show that the out-of-control performance of the explicit formulas was excellent in all cases studied, thereby making it a good alternative to the well-established NIE method that requires only a fraction of a second to compute the result.

Table 1 The out-of-control ARL obtained using the explicit formulas and NIE methods for detecting changes in the mean of a SARFIMA(1, $d=0.25,1$) \times (1, $D=0.1,1$)₁₂ process running on a CUSUM control chart

k	2.5		%	3.5		%	4.5		%
	h	4.14452		2.793457	1.728737				
δ	Explicit	NIE	Accuracy	Explicit	NIE	Accuracy	Explicit	NIE	Accuracy
0.025	312.991 (<0.001)	312.326 (1891.08)	99.79	318.335 (<0.001)	317.817 (1878.09)	99.84	319.705 (<0.001)	319.374 (1894.17)	99.90
0.05	266.903 (<0.001)	266.359 (1895.25)	99.80	275.818 (<0.001)	275.382 (1881.95)	99.84	278.149 (<0.001)	277.869 (1906.02)	99.90
0.10	198.424 (<0.001)	198.052 (1881.76)	99.81	211.082 (<0.001)	210.767 (1897.74)	99.85	214.524 (<0.001)	214.318 (1879.67)	99.90
0.25	94.464 (<0.001)	94.324 (1877.72)	99.85	107.407 (<0.001)	107.269 (1898.30)	99.87	111.304 (<0.001)	111.211 (1883.39)	99.92
0.50	38.947 (<0.001)	38.907 (1891.45)	99.90	46.971 (<0.001)	46.923 (1883.25)	99.90	49.739 (<0.001)	49.706 (1902.31)	99.93
0.75	21.223 (<0.001)	21.207 (1892.41)	99.92	26.057 (<0.001)	26.036 (1876.08)	99.92	27.915 (<0.001)	27.900 (1892.67)	99.95
1	13.732 (<0.001)	13.724 (1910.41)	99.94	16.798 (<0.001)	16.787 (1909.98)	99.93	18.085 (<0.001)	18.076 (1909.77)	99.95
2	5.382 (<0.001)	5.381 (1918.56)	99.98	6.159 (<0.001)	6.157 (1914.38)	99.97	6.581 (<0.001)	6.579 (1917.78)	99.97
3	3.502 (<0.001)	3.502 (1901.44)	100.00	3.800 (<0.001)	3.799 (1916.86)	99.97	3.996 (<0.001)	3.996 (1919.56)	100.00
4	2.729 (<0.001)	2.729 (1902.52)	100.00	2.867 (<0.001)	2.867 (1935.77)	100.00	2.978 (<0.001)	2.977 (1914.58)	99.97
5	2.316 (<0.001)	2.316 (1915.45)	100.00	2.386 (<0.001)	2.386 (1913.94)	100.00	2.455 (<0.001)	2.455 (1936.55)	100.00

Note: The numerical results in parentheses are computational times in seconds

Table 2 The out-of-control ARL obtained using the explicit formulas and NIE methods for detecting changes in the mean of a SARFIMA(1, $d = 0.35$, 1) \times (1, $D = 0.1$, 1)₁₂ process running on a CUSUM control chart

k	2.5		%	3.5		%	4.5		%
	3.54245			2.369346			1.334222		
h	Explicit	NIE	Accuracy	Explicit	NIE	Accuracy	Explicit	NIE	Accuracy
0.025	316.091 (<0.001)	315.470 (1914.09)	99.80	319.068 (<0.001)	318.621 (1881.13)	99.86	319.909 (<0.001)	319.653 (1888.83)	99.92
0.05	272.049 (<0.001)	271.532 (1918.39)	99.81	277.062 (<0.001)	276.685 (1880.22)	99.86	278.503 (<0.001)	278.284 (1878.99)	99.92
0.10	205.659 (<0.001)	205.294 (1883.02)	99.82	212.907 (<0.001)	212.632 (1881.77)	99.87	215.055 (<0.001)	214.895 (1889.30)	99.93
0.25	101.666 (<0.001)	101.516 (1876.44)	99.85	109.436 (<0.001)	109.315 (1878.97)	99.89	111.942 (<0.001)	111.869 (1884.36)	99.93
0.50	43.246 (<0.001)	43.197 (1885.28)	99.89	48.378 (<0.001)	48.335 (1887.42)	99.91	50.229 (<0.001)	50.203 (1868.09)	99.95
0.75	23.731 (<0.001)	23.711 (1892.08)	99.92	26.983 (<0.001)	26.983 (1875.42)	100.00	28.264 (<0.001)	28.252 (1876.34)	99.96
1	15.278 (<0.001)	15.268 (1917.11)	99.93	17.428 (<0.001)	17.418 (1912.09)	99.94	18.338 (<0.001)	18.331 (1912.27)	99.96
2	5.738 (<0.001)	5.736 (1919.80)	99.97	6.357 (<0.001)	6.355 (1913.77)	99.97	6.675 (<0.001)	6.673 (1918.53)	99.97
3	3.625 (<0.001)	3.625 (1927.78)	100.00	3.889 (<0.001)	3.889 (1909.09)	100.00	4.043 (<0.001)	4.043 (1911.09)	100.00
4	2.779 (<0.001)	2.779 (1907.20)	100.00	2.916 (<0.001)	2.916 (1910.11)	100.00	3.006 (<0.001)	3.005 (1895.03)	99.97
5	2.336 (<0.001)	2.336 (1904.30)	100.00	2.416 (<0.001)	2.416 (1900.99)	100.00	2.474 (<0.001)	2.473 (1876.36)	99.96

Note: The numerical results in parentheses are computational times in seconds

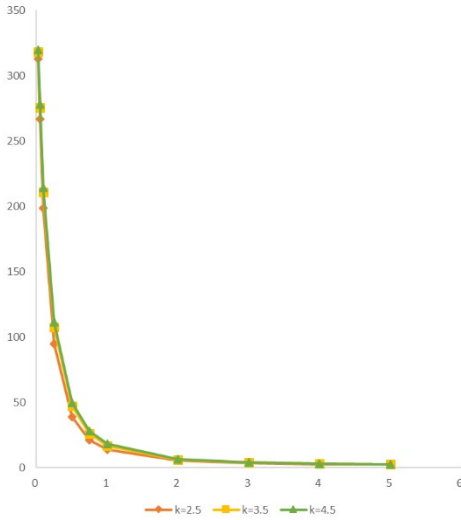
Table 3 The out-of-control ARL obtained using the explicit formulas and NIE methods for detecting changes in the mean of a SARFIMA(1, $d = 0.45$, 1) \times (1, $D = 0.1$, 1)₁₂ process running on a CUSUM control chart

k	2.5		%	3.5		%	4.5		%
	4.343651			2.908201			1.832392		
h	Explicit	NIE	Accuracy	Explicit	NIE	Accuracy	Explicit	NIE	Accuracy
0.025	311.604 (<0.001)	310.938 (1881.59)	99.79	318.079 (<0.001)	317.543 (1901.33)	99.83	319.631 (<0.001)	319.281 (1871.58)	99.89
0.05	264.621 (<0.001)	264.081 (1882.94)	99.80	275.386 (<0.001)	274.935 (1900.45)	99.84	278.024 (<0.001)	277.727 (1886.52)	99.89
0.10	195.265 (<0.001)	194.902 (1893.06)	99.81	210.454 (<0.001)	210.128 (1874.88)	99.85	214.334 (<0.001)	214.117 (1898.13)	99.90
0.25	91.446 (<0.001)	91.315 (1890.22)	99.86	106.721 (<0.001)	106.581 (1884.95)	99.87	111.079 (<0.001)	110.983 (1899.55)	99.91
0.50	37.244 (<0.001)	37.209 (1895.05)	99.91	46.508 (<0.001)	46.460 (1896.50)	99.90	49.572 (<0.001)	49.536 (1868.97)	99.93
0.75	20.275 (<0.001)	20.262 (1871.09)	99.94	25.759 (<0.001)	25.738 (1895.84)	99.92	27.798 (<0.001)	27.781 (1886.30)	99.94
1	13.171 (<0.001)	13.165 (1899.72)	99.95	16.598 (<0.001)	16.587 (1903.14)	99.93	18.001 (<0.001)	17.992 (1921.73)	99.95
2	5.272 (<0.001)	5.271 (1894.23)	99.98	6.099 (<0.001)	6.097 (1935.39)	99.97	6.551 (<0.001)	6.549 (1904.39)	99.97
3	3.471 (<0.001)	3.471 (1927.14)	100.00	3.774 (<0.001)	3.773 (1890.55)	99.97	3.981 (<0.001)	3.981 (1931.86)	100.00

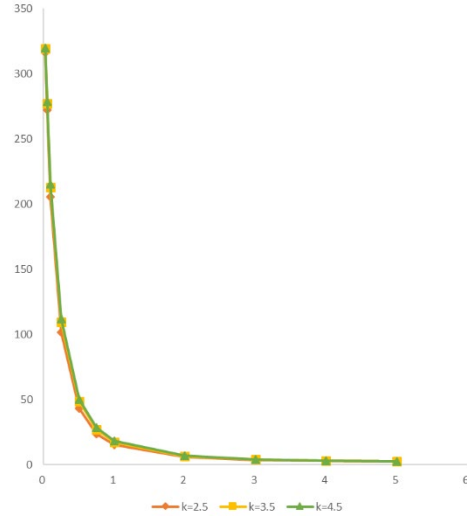
Table 3 (Continued)

k	2.5		%	3.5		%	4.5		%
	Explicit	NIE		Explicit	NIE		Explicit	NIE	
h	4.343651			2.908201			1.832392		
δ	Explicit	NIE	Accuracy	Explicit	NIE	Accuracy	Explicit	NIE	Accuracy
4	2.721 (<0.001)	2.721 (1929.17)	100.00	2.854 (<0.001)	2.853 (1914.78)	99.96	2.969 (<0.001)	2.969 (1924.81)	100.00
5	2.316 (<0.001)	2.316 (1893.14)	100.00	2.378 (<0.001)	2.378 (1926.86)	100.00	2.450 (<0.001)	2.450 (1896.09)	100.00

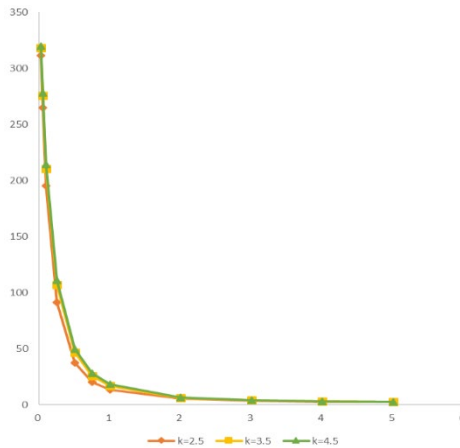
Note: The numerical results in parentheses are computational times in seconds



(a) $ARFIMA(1, 0.25, 1) \times (1, 0.1, 1)_{12}$



(b) $ARFIMA(1, 0.35, 1) \times (1, 0.1, 1)_{12}$



(c) $ARFIMA(1, 0.45, 1) \times (1, 0.1, 1)_{12}$

Figure 2 Graphical representation of the out-of-control performance of the ARL derivations using the explicit formulas to detect shifts in the mean of various $SARFIMA(p, d, q) \times (P, D, Q)_{12}$ models running on a CUSUM control chart

6. Illustrative Example

Two real datasets suitable for SARFIMA(p, d, q) \times (P, D, Q) $_s$ processes with exponential white noise were used to illustrate the performance of the proposed method. The two datasets and parameters for the SARFIMA(p, d, q) \times (P, D, Q) $_s$ process were fitted by using statistical software package Eviews 10. After that, testing whether the white noise in the model is exponentially distributed was checked using the Kolmogorov-Smirnov test in statistical software package SPSS, the p-values for which are reported in Table 4.

Table 4 The estimated parameters and test white noise for fitting the SARFIMA(p, d, q) \times (P, D, Q) $_{12}$ model of the real dataset

Parameter	First data set			Second data set		
	Coefficient	t-Statistic	Prob.	Coefficient	t-Statistic	Prob.
d	0.353493	8144.855	0.0000	0.353979	2.0163	0.0467
D	0.436033	7.868902	0.0000	0.003199	3.6880	0.0004
ϕ	0.813983	2361.708	0.0000	0.951845	5.2054	0.0000
θ_1	1.000000	49614.13	0.0000	-0.905111	-3.5982	0.0005
Φ_1	-0.326066	-509.8818	0.0000	0.999825	682.3432	0.0000
Θ_1	-0.999784	-7231.985	0.0000	-0.910858	-2.5720	0.0117

Testing whether the white noise is exponentially distributed.		
	First data set	Second data set
Exponential Parameter (ν)	1,544.3984	97,353.7145
Kolmogorov-Smirnov	0.968	1.060
Asymptotic Significance (2-Sided)	0.306	0.211

*A significance level of 0.05.

6.1. The first dataset: road traffic accidents in Thailand

Real data on the number of people involved in road accidents in Thailand from April 2015 to February 2022 comprising 83 monthly observations were downloaded from the moph.go.th website. The data fit a SARFIMA(1,0.353493,1) \times (1,0.436033,1) $_{12}$ model with the following coefficient parameters: $\hat{\phi} = 0.813983$, $\hat{\theta}_1 = 1$, $\hat{\Phi}_1 = -0.326066$, $\hat{\Theta}_1 = -0.999784$.

Moreover, the white noise followed an exponential distribution (Kolmogorov-Smirnov test = 0.968 and p-value = 0.306; i.e., statistically nonsignificant (p-value<0.05)) with a mean of 1,544.3984. Hence, the fitted SARFIMA(1,0.353493,1) \times (1,0.436033,1) $_{12}$ model is

$$(1 - 0.813983B)(1 + 0.326066B^{12})(1 - B)^{0.353493}(1 - B^{12})^{0.436033} X_t = (1 - B)(1 + 0.999784B^{12})\varepsilon_t \tag{20}$$

or

$$\begin{aligned} X_t = & \varepsilon_t - \varepsilon_{t-1} + 0.999784\varepsilon_{t-12} - 0.999784\varepsilon_{t-13} - 1.167476X_1 - 0.173469X_2 - 0.030298X_3 \\ & - 0.051048X_4 + 0.109967X_{12} - 0.926855X_{13} + 0.041335X_{14} + 0.030677X_{15} - 0.016645X_{16} \\ & + 0.185639X_{24} - 0.207813X_{25} + 0.022666X_{26} + 0.004489X_{27} + 0.078271X_{36} - 0.068721X_{37} \\ & - 0.025676X_{38} + 0.022432X_{39} + 0.003272X_{40} + 0.020900X_{48} - 0.017013X_{49} - 0.009776X_{50} \\ & + 0.006647X_{51} + 0.001067X_{52} \end{aligned} \tag{21}$$

where $\varepsilon_t \sim \text{Exp}(\lambda_0 = 1,544.3984)$.

6.2. The second dataset: orchid exports from Thailand

The export value of fresh orchid flowers from January 2012 to January 2020 comprising 97 monthly observations was obtained from oae.go.th. The SARFIMA(p, d, q) \times (P, D, Q)₁₂ process was found to be suitable for this dataset. Table 4 provides the coefficient parameters: $\hat{\phi}_1 = 0.951845$, $\hat{\theta}_1 = -0.905111$, $\hat{\Phi}_1 = 0.999825$, $\hat{\Theta}_1 = -0.910858$. Moreover, the exponential white noise had a mean of 97,353.7145. Hence, the fitted SARFIMA(1,0.353979,1) \times (1,0.003199,1)₁₂ model is

$$(1 - 0.951845B)(1 - 0.999825B^{12})(1 - B)^{0.353979}(1 - B^{12})^{0.003199} X_t = (1 + 0.905111B)(1 + 0.910858B^{12})\varepsilon_t$$

or

$$\begin{aligned} X_t = & 0.905111\varepsilon_t - \varepsilon_{t-1} + 0.910858\varepsilon_{t-12} - 0.824428\varepsilon_{t-13} + 1.305824X_1 - 0.22259X_2 - 0.046098X_3 \\ & - 0.059713X_4 + 1.003024X_{12} - 1.310140X_{13} + 0.2232675X_{14} + 0.046438X_{15} + 0.0597033X_{16} \\ & - 0.002443X_{24} + 0.0036403X_{25} - 0.000995X_{26} + 0.0006168X_{27} + 0.000496X_{36} - 0.0002731X_{37} \\ & - 0.000404X_{38} + 0.0001378X_{39} + 0.000063X_{40} - 0.001061X_{48} + 0.001009X_{49} + 0.0004969X_{50} \\ & - 0.000049X_{51} - 0.000421X_{52} \end{aligned} \tag{22}$$

where $\varepsilon_t \sim \text{Exp}(\lambda_0 = 97,353.7145)$.

We applied the explicit formulas and the NIE method from (16) and (18), respectively, with $ARL_0 = 370$. The parameter values consistent with $k = 2.5$ combined with $UCL(h)$ calculated using (16) are reported in Table 5.

The out-of-control ARL_1 results using both the proposed and NIE methods were similar for a shift size of 0.025, 0.05, 0.10, 0.25, 0.50, 0.75, 1, 2, 3, 4, or 5 (Table 5). Once again, there was excellent agreement between the two methods and the proposed explicit formulas method was very accurate. In addition, the ARL results were the same as those in Tables 1–3. Moreover, the explicit formulas were compared with SDRL benchmarks (Table 5). It was found that ARL and SDRL results also show a decreasing pattern as the shift size is increased for both real datasets. Figure 3(a) shows the control limits for the SARFIMA(p, d, q) \times (P, D, Q)₁₂ process comprising the dataset of road accident patients in Thailand running on a CUSUM control chart, which are $LCL = 0$, $CL = 1,544.3984$, and $UCL = 2,000.938$. The first out-of-control signal can be observed at the 5th observation. Similarly, Figure 3(b) shows the control limits for the SARFIMA(p, d, q) \times (P, D, Q)₁₂ process comprising the second dataset running on a CUSUM control chart, which are $LCL = 0$, $CL = 97,353.7145$, and $UCL = 107,103$. This time, the first out-of-control signal occurs at the 4th observation.

6. Conclusions

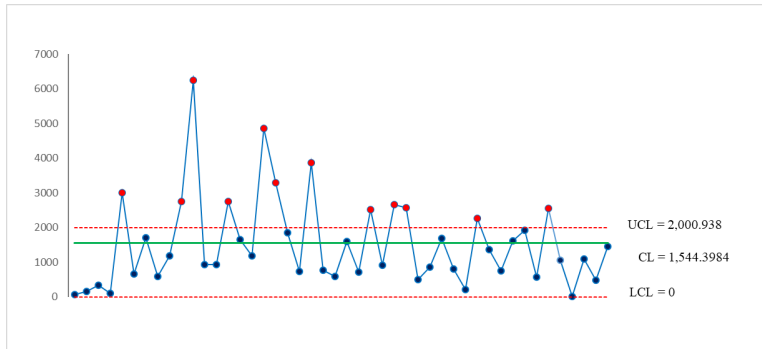
A derivation of the ARL using explicit formulas to detect shifts in the mean of a SARFIMA(p, d, q) \times (P, D, Q)₁₂ process with exponential white noise running on a CUSUM control chart was proposed. Its performance was compared numerically with the well-known NIE method using processes involving both simulated and real-life data. Although their ARL_1 results were very similar, the computation time using the explicit formulas was far less than for the NIE method. Since developing explicit formulas, the computation formula is more straightforward and can be completed in one step. Therefore, the proposed explicit formulas method could be used in place of the NIE method. For comparison, we computed the SDRL in addition to the ARL , employing both the explicit

formula and the NIE method. A rapid and the same direction in the ARL_1 and $SDRL_1$ values was detected. The implementation of these measurement methods has been explained via real data sets. Although our current interest was only in seasonal processes running on the CUSUM control chart, future work could extend to designing other control charts that utilize past data to improve the detection of small-to-moderate shifts in process parameters, focusing on memory-type charts, such as the EWMA control chart. It would also be interesting to apply our method to models involving exogenous variables, such as ARIMAX, ARFIMAX, etc. These works are currently in progress.

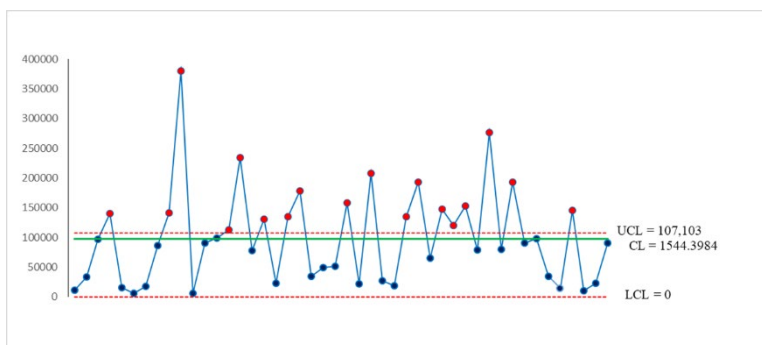
Table 5 The out-of-control ARL results for detecting changes in the mean of a $SARFIMA(p, d, q) \times (P, D, Q)_{12}$ model with real data running on a CUSUM control chart obtained using the explicit formulas and NIE methods

		First data set			Second data set			
k	2.5			2.5				
h	2,000.938			%Accuracy	107,103			%Accuracy
δ	ARL		SDRL		ARL		SDRL	
	Explicit	NIE			Explicit	NIE		
0.025	320.126 (<0.001)	319.927 (1872.11)	319.626	99.94	320.188 (<0.001)	319.976 (1867.03)	319.688	99.93
0.05	278.885 (<0.001)	278.716 (1873.74)	278.385	99.94	278.993 (<0.001)	278.812 (1867.91)	278.493	99.94
0.10	215.664 (<0.001)	215.539 (1867.77)	215.163	99.94	215.827 (<0.001)	215.694 (1873.84)	215.326	99.94
0.25	112.793 (<0.001)	112.735 (1864.35)	112.292	99.95	112.994 (<0.001)	112.934 (1871.88)	112.493	99.95
0.50	51.055 (<0.001)	51.033 (1875.44)	50.553	99.96	51.215 (<0.001)	51.192 (1878.07)	50.713	99.96
0.75	28.984 (<0.001)	28.973 (1869.92)	28.480	99.96	29.101 (<0.001)	29.090 (1884.14)	28.597	99.96
1	18.962 (<0.001)	18.958 (1897.25)	18.455	99.98	19.049 (<0.001)	19.043 (1882.13)	18.542	99.97
2	7.067 (<0.001)	7.065 (1902.17)	6.548	99.97	7.101 (<0.001)	7.100 (1881.03)	6.582	99.99
3	4.326 (<0.001)	4.325 (1891.27)	3.793	99.98	4.344 (<0.001)	4.344 (1879.52)	3.811	100.00
4	3.227 (<0.001)	3.227 (1892.32)	2.681	100.00	3.237 (<0.001)	3.237 (1883.28)	2.691	100.00
5	2.655 (<0.001)	2.655 (1894.22)	2.096	100.00	2.662 (<0.001)	2.662 (1874.29)	2.103	100.00

Note: The numerical results in parentheses (-) are computational times in seconds



(a)



(b)

Figure 3 Control limits for the $SARFIMA(p, d, q) \times (P, D, Q)_{12}$ processes comprising (a) the first real dataset and (b) the second real dataset running on a CUSUM control chart using the proposed explicit formulas for $ARL_0 = 370$

Acknowledgements

This research was funded by Thailand Science Research and Innovation Fund (NSRF) and King Mongkut's University of Technology North Bangkok with Contract no. KMUTNB-FF-66-62.

References

- Areepong Y, Peerajit W. Integral equation solutions for the average run length for monitoring shifts in the mean of a generalized seasonal $ARFIMAX(P, D, Q, r)_s$ process running on a CUSUM control chart. PLoS ONE. 2022; 17(2), e0264283.
- Atkinson K, Han W. Theoretical Numerical Analysis: A Functional Analysis Framework. New York: Springer Verlag; 2001.
- Atienza OO, Tang LC, Ang BW. A CUSUM scheme for autocorrelated observations. J Qual Technol. 2002; 34(2): 187-199.
- Bisognin C, Lopes S.R.C. Properties of seasonal long memory processes, Math Comput Model. 2009; 49: 1837-1851.
- Brook D, Evans DA. An Approach to the probability distribution of CUSUM run length. Biometrika. 1972; 9: 539-548.
- Bualuang D, Peerajit W. Performance of the cusum control chart using approximation to arl for long-memory fractionally integrated autoregressive process with exogenous variable. Appl Sci Eng Prog. 2022; 16(2): 1-13.

- Champ CW, Rigdon SE. A comparison of the Markov chain and the integral equation approaches for evaluating the run length distribution of quality control charts. *Commun Stat Simul Comput.* 1991; 20(1): 191-203.
- Chang YM, Wu TL. On average run lengths of control charts for autocorrelated processes. *Methodol Comput Appl Probab.* 2011; 13: 419-431.
- Contreras-Reyes JE, Palma W. Statistical analysis of autoregressive fractionally integrated moving average models in R. *Comput Stat.* 2013; 28(5): 2309-2331.
- Fu MC, Hu JQ. Efficient design and sensitivity analysis of control charts using Monte Carlo simulation. *Manag Sci.* 1999; 45(3): 395-413.
- Granger CWJ, Joyeux R. An introduction to long memory time series models and fractional differencing. *J Time Ser Anal.* 1980; 1(1): 15-29.
- Hawkins DM, Wu Q. The CUSUM and the EWMA Head-to-Head. *Qual Eng.* 2014; 26(2): 215-222.
- Hosking JRM. Fractional differencing. *Biometrika.* 1981; 68(1): 165-176.
- Hosking, JRM. Modelling persistence in hydrological time series using fractional differencing. *Water Resour Res.* 1984; 20(12): 1898-1908.
- Lucas JM, Crosier RB. Fast initial response for CUSUM quality-control schemes: Give your CUSUM a head start. *Technometrics.* 1982; 24: 199-205.
- Montanari A, Rosso R, Taqqu MS. A seasonal fractional ARIMA model applied to the Nile river monthly flows at Aswan. *Water Resour Res.* 2000; 36(5): 1249-1259.
- Montgomery DC. *Introduction to Statistical Quality Control.* New York: John Wiley and Sons; 2004.
- Ooms M. Flexible seasonal long memory and economic time series, Preprint of the Econometric Institute, Erasmus University. Rotterdam; 1995.
- Page ES. Continuous inspection schemes. *Biometrika.* 1954; 41(1-2): 100-115.
- Palma W. *Long-Memory Time Series - Theory and Methods.* John Wiley. New Jersey; 2007.
- Peerajit W, Cumulative Sum Control Chart Applied to Monitor Shifts in the Mean of a Long-memory ARFIMAX(p, d^*, q, r) Process with Exponential White Noise. *Thail Stat.* 2022; 20(1): 144-161.
- Peerajit W, Areepong Y. Alternative to detecting changes in the mean of an autoregressive fractionally integrated process with exponential white noise running on the modified EWMA control chart. *Processes.* 2023; 11(2): 503-525,
- Peerajit W. Developing Average Run Length for Monitoring Changes in the Mean on the Presence of Long Memory under Seasonal Fractionally Integrated MAX Model. *Math Stat.* 2023; 11(1): 34-50.
- Phantu, S., Areepong, Y., Sukparungsee, S. Average Run Length Formulas for Mixed Double Moving Average-Exponentially Weighted Moving Average Control Chart. *Sci Technol Asia.* 2023; 28(1): 77-89
- Porter-Hudak S. An application of the seasonal fractionally differenced model to the monetary aggregates. *J Am Stat Assoc.* 1990; 85(410): 338-344.
- Robert SW. Control chart test based on geometric moving averages. *Technometrics.* 1959; 42: 239-250.
- Ray BK. Long-range forecasting of IBM product revenues using a seasonal fractionally differenced ARMA model. *Int J Forecast.* 1993;9: 255-269.
- Saengsura, N., Sukparungsee, S., Areepong, Y. A Mixed TCC Cumulative Sum-Double Moving Average Control Chart For Detecting Mean Shifts Under Symmetric And Asymmetric Distributions, *J Appl Sci Eng.* 2024; 27(10): 3337-3347.
- Shewhart, WA. *Economic control of quality of manufactured product.* American Society for Quality Control. Milwaukee, Wis; 1980.

- Sukparungsee S, Areepong Y. An explicit analytical solution of the average run length of an exponentially weighted moving average control chart using an autoregressive model. *Chiang Mai J Sci.* 2017; 44(3): 1172-1179.
- Sunthornwat R, Areepong Y. Average run length on CUSUM control chart for seasonal and non-seasonal moving average processes with exogenous variables. *Symmetry.* 2020; 12(1): 1-15.
- Sunthornwat R, Areepong Y. Evaluating the Performance of Modified EWMA Control Schemes for Serially Correlated Observations. *Thail Stat.* 2024; 22(3): 657-673.
- Sunthornwat R, Sukparungsee S, Areepong Y. The Development and Evaluation of Homogenously Weighted Moving Average Control Chart based on an Autoregressive Process. *HighTech and Innovation Journal.* 2024; 5(1): 16-35.
- Suparman S. A new estimation procedure using a reversible jump MCMC algorithm for AR models of exponential white noise. *Int J GEOMATE.* 2018; 5(15): 85-91.
- Vanbrackle LN, Reynolds MR. EWMA and CUSUM control charts in the presence of correlation. *Commun Stat Simul Comput.* 1997;(26)3: 979-1008.
- Woodall WH. On the markov chain approach to the two-sided CUSUM procedure. *Technometrics.* 1984; 26(1): 41-46.
- Zacks S. The probability distribution and the expected value of a stopping variable associated with one-sided CUSUM procedures for non-negative integer valued random variables. *Commun Stat - Theory Methods.* 1981; 10(21): 2245-2258.
- Zwetsloot IM, Woodall WH. A head-to-head comparative study of the conditional performance of control charts based on estimated parameters. *Qual Eng.* 2017; 29(2): 244-253.